Trans-splicing vectors expand the utility of adeno-associated virus for gene therapy

Ziying Yan*, Yulong Zhang*, Dongsheng Duan*†, and John F. Engelhardt*†‡§

†Center for Gene Therapy of Cystic Fibrosis and Other Genetic Diseases, and Departments of *Anatomy and Cell Biology and ‡Internal Medicine, University of Iowa College of Medicine, Iowa City, IA 52242

Edited by Kenneth I. Berns, University of Florida, Gainesville, FL, and approved March 23, 2000 (received for review January 5, 2000)

Adeno-associated viral (AAV) vectors have demonstrated considerable promise for gene therapy of inherited diseases. However, with a packaging size of <5 kb, applications have been limited to relatively small disease genes. Based on the finding that AAV genomes undergo intermolecular circular concatamerization after transduction in muscle, we have developed a paradigm to increase the size of delivered transgenes with this vector through trans-splicing between two independent vectors coadministered to the same tissue. When two vectors encoding either the 5′ or 3′ portions of the erythropoietin genomic locus were used, functional erythropoietin protein was expressed in muscle subsequent to the formation of intermolecular circular concatamers in a head-to-tail orientation through trans-splicing between these two independent vector genomes. These findings will allow for the application of AAV technologies to a wider variety of diseases for which therapeutic transgenes exceed the packaging limitation of present AAV vectors.

Adeno-associated virus (AAV) is a single-stranded DNA parvovirus with a helper-dependent life cycle. This virus has attracted considerable interest as a vector for gene therapy because of certain inherent aspects of its life cycle. These aspects include its potential for site-specific integration at the AAVS1 locus, its nonpathogenicity as a helper-dependent virus, and its ability to infect nondividing cells (1–3). With the promise of recombinant AAV (rAAV) vectors for muscle-directed therapies, a renewed interest in investigating the mechanisms of rAAV transduction in this tissue has emerged. Of foremost interest is the question why muscle tissue appears to be so tropic for this virus. Several important findings have recently emerged from studies in this area. First, the AAV-2 cell membrane receptor, heparan sulfate proteoglycan, as well as two coreceptors, fibroblast growth factor receptor-1 (FGFR-1) and $\alpha_V\beta_5$ integrin, have been identified (4–6). Second, it has been shown that latent phase infection of muscle with rAAV involves the conversion of the single-stranded viral DNA to circular intermediate forms that correlate with long-term transgene expression (7–9). Circular intermediate formation and transgene persistence are intricately linked to a concatamerization process, which is controlled, at least in part, by intermolecular recombination between independent viral genomes (7, 10).

Despite our increased understanding of rAAV transduction biology, the application of this vector in treating disease has been limited by the fundamental aspects of rAAV biology that define its packaging limits. Thus, diseases caused by defective genes larger than 5 kb, such as factor VIII deficiency or Duchenne muscular dystrophy, cannot presently be approached with this vector system. In this report, we describe a strategy permitting the delivery of large transgenes that exceed the normal packaging size of rAAV. This approach entails the coadministration of two independent trans-splicing rAAV vectors encoding distinct segments of a large therapeutic gene and intron donor and acceptor signals. The design of this approach was based on the current understanding that rAAV vectors readily undergo a concatamerization process through intermolecular recombination from circular monomer intermediates of the viral genome (10). In this report, we demonstrate that this dual vector, trans-splicing strategy can result in the functional expression of therapeutic levels of protein from the erythropoietin (Epo) genomic locus. These findings will greatly broaden the application of rAAV vectors for gene therapies to muscle, as well as to other organs and tissues having circular concatamerization as an inherent part of the rAAV life cycle.

Materials and Methods

Production of Recombinant Viral Vectors. A 2.4-kb *Bst*EII/*Bgl*II human genomic DNA fragment encoding the entire Epo gene was cloned from a lambda phage human genomic library (CLONTECH). This fragment was inserted into the multiple cloning site of pIRES2-EGFP (CLONTECH) to generate pEpoEGFP, which expresses both Epo and enhanced green fluorescent protein (EGFP) from a single transcript. By cutting at a unique *Bcl*I site within a central intron of the Epo gene, the Epo genomic locus was divided into two parts and inserted into two independent rAAV vectors by using pSub201 (11) as the source of inverted terminal repeats (ITRs). These proviral plasmids, termed pCisAV.Epo1 and pCisAV.Epo2, were used to produce recombinant viruses (Fig. 1) to study the intermolecular trans-splicing production of Epo mRNA and protein. Additionally, to evaluate the efficiency of transcription through the ITR, a double-D ITR sequence (9) was cloned into Epo intron 3 of pEpoEGFP to generate the plasmid pEpo(ITR)EGFP. rAAV stocks were generated and purified as previously described (12, 13). The particle titer of both viruses, determined by slot blotting against plasmid standards, was typically 1×10^{12} particles per ml. The level of contaminating helper adenovirus and wild-type AAV2 was determined as previously described (7) and was less than one functional particle per 1×10^{10} particles of rAAV.

***In Vitro* Analysis of Trans-Splicing in Primary Fibroblasts.** Fetal fibroblasts grown in 10% FCS/DMEM were plated on six-well plates at a density of 8×10^5 cells per well the day before infection with AV.Epo1 and/or AV.Epo2 (multiplicity of infection = 10^4 particles per cell). Human Epo (hEpo) expression was assayed by ELISA using the hEpo Quantikine IVD kit from R&D Systems, according to the manufacturer's recommendations. The level of hEpo secreted from transduced cells during a 24-h period was tested at 2, 3, 5, 7, and 10 days after infection. Production of full-length hEpo protein was assessed by immunoprecipitation and Western blot analysis as follows. One milliliter of culture medium from the transduced cells was incubated with 1 μg of rabbit polyclonal anti-human Epo Ab (R&D Systems), followed with 20 μl of

This paper was submitted directly (Track II) to the PNAS office.

Abbreviations: AAV, adeno-associated virus; rAAV, recombinant AAV; Epo, erythropoietin; hEpo, human Epo; Amp^r, ampicillin resistance; Kan^r, kanamycin resistance; EGFP, enhanced green fluorescent protein; ITR, inverted terminal repeat.

See commentary on page 6239.

§To whom reprint requests should be addressed at: Department of Anatomy and Cell Biology, University of Iowa College of Medicine, 51 Newton Road, Room 1-111 BSB, Iowa City, IA 52242. E-mail: john-engelhardt@uiowa.edu.

The publication costs of this article were defrayed in part by page charge payment. This article must therefore be hereby marked "*advertisement*" in accordance with 18 U.S.C. §1734 solely to indicate this fact.

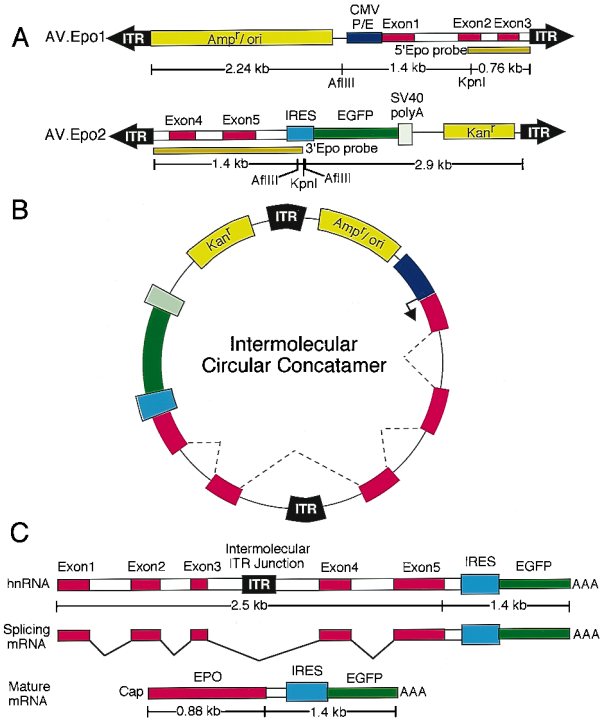

Fig. 1. Structure of rAAV vectors and strategy used to generate trans-splicing vectors expressing functional human Epo. Two rAAV vectors, AV.Epo1 and AV.Epo2, encoding either the 5′ or 3′ genomic segment of the human Epo gene, and the diagnostic restriction enzyme sites used to characterize the structure of circular intermediates are shown in *A*. Additional elements, kanamycin resistance (Kan^r), ampicillin resistance (Amp^r), and a bacterial replication origin (ori) were included to allow for molecular characterization of circular concatamers after bacterial rescue from muscle DNA extracted by the Hirt procedure. An internal ribosome entry site (IRES) sequence and the EGFP transgene were also incorporated into the 3′ end of the Epo transcript to allow for direct visualization of transgene expression after concatamerization. The locations of 5′ and 3′ Epo DNA probes used for structural analysis in Fig. 4 are marked below each viral construct. (*B*) Expected structure of a circular concatamer arising from intermolecular recombination that would allow for functional trans-splicing of Epo message. The expected splicing patterns are denoted by dashed lines. (*C*) Expected heterogeneous nuclear RNA, splicing pattern, and mature mRNA transcripts resulting from circular concatamerization.

protein-A agarose. The pellets were washed four times with RIPA buffer (0.15 mM NaCl/0.05 mM Tris·HCl, pH 7.2/1% Triton X-100/1% sodium deoxycholate/0.1% SDS) and resolved on a 12% SDS/PAGE gel. Western blots were probed individually with goat anti-Epo polyclonal Ab (Santa Cruz Biotechnology), which recognized the Epo N terminus, and a mouse anti-human Epo mAb directed at the C terminus. After incubation with appropriate horseradish peroxidase-labeled secondary Abs, the full-length Epo protein was visualized via the ECL system (Amersham Pharmacia). To confirm transcription and splicing of mRNA through the predicted junctional ITR region, mRNA was extracted from fetal fibroblasts infected with single or dual vectors by using a MicroFastTrack 2.0 mRNA kit (Invitrogen). As a control, mRNA was also prepared from fetal fibroblasts that were transfected with pEpoEGFP. Northern blots of these mRNA samples were hybridized with ^{32}P-labeled hEpo or EGFP probes and exposed to film.

***In Vivo* Analysis of Trans-Splicing in Muscle.** The tibialis anterior muscles of 4- to 5-wk-old C57BL6 mice were injected twice with 30 μl of recombinant virus in Hepes-buffered saline on day 0 and day 3. The total virus administration in the low dosage group ($n = 12$) was 6×10^{10} combined particles of AV.Epo1 and AV.Epo2 per muscle, and, in the high dosage group ($n = 4$), 4×10^{11} viral particles were injected per muscle. The two viruses were mixed in a ratio of 1:1 for the coinfection group. Age-matched control mice for both the high and low dose groups ($n = 4$ for each dose) were injected with an equivalent dose of AV.Epo1 in the right tibialis muscle, and AV.Epo2 in the left tibialis muscle. Additionally, age-matched uninfected animals were also evaluated for each dosage group ($n = 4$ for each group). The full-length functional Epo protein produced by infected mice was monitored by analysis of the biological effect of Epo on the hematocrit. Blood samples were taken at various time points by retroorbital bleed by using heparin-coated capillary tubes. After centrifugation, hematocrits were determined in an IEC microcapillary reader. Additionally, hEpo levels in the serum samples were determined by ELISA (R&D Systems) as described above. To evaluate the overall efficiency of the intermolecular trans-splicing in muscle tissue *in situ*, anterior tibialis muscles infected individually or with both Epo vectors were harvested at 150 days postinfection, and EGFP transgene expression was evaluated directly by fluorescence microscopy. To perform detailed analysis of the viral genome concatamerization process, Hirt DNA was prepared from 110- and 150-day muscle samples ($n = 3$ for each time point) as previously described (7, 10), and one-tenth of the Hirt DNA from each independent muscle sample was transformed into DH10B (GIBCO) *Escherichia coli* strain and selected for Amp^r. The total number of Amp^r colonies was calculated for each muscle sample, and the fraction of these colonies that were also Kan^r was tested by replica plating (100 colonies tested per muscle sample). Additionally, 100 rescued colonies from each muscle sample were evaluated by hybridization against 5′ and 3′ Epo probes that originated from AV.Epo1 and AV.Epo2, respectively (see Fig. 1 for probe location). Restriction mapping and Southern blotting with a comprehensive set of probes (See Fig. 4 for details) were used to characterize the structure of 10 rescued Amp^r clones (which hybridized only to the 5′ Epo probe) and 92 rescued Amp/Kan coresistant intermolecular concatamers (which hybridized to both 5′ and 3′ Epo probes). These data were then correlated with the ability of rescued plasmids to express both Epo and EGFP after transfection into HeLa cells. In this functional assay, Epo was evaluated by cotransfecting 0.5 μg of rescued circular intermediates with 0.5 μg of pCMVLuciferase control plasmid into 70% confluent HeLa cells. At 24 h posttransfection, 2 μl of culture medium was used for the determination of Epo expression by ELISA. Values of Epo production were normalized to luciferase activity in cell lysates.

Renal Failure-Induced Anemia in Mice. Renal failure anemia was induced in mice by adenine administration at a dosage of 25 μg per gram body weight per day. Adenine or placebo pellets (15 mg/21 days release, Innovative Research of America) were implanted s.c. into the flanks of the mice. Adenine tablets were implanted at 35 and 100 days postinfection in animals ($n = 4$) coinfected with low doses (6×10^{10} particles) of both AV.Epo1 and AV.Epo2 viruses. Uninfected, age-matched control animals were also implanted with both adenine and placebo tablets ($n = 4$ for each group). Hematocrit was monitored as described above, and renal histopathology was assessed in paraffin-embedded hematoxylin/eosin (H&E)-stained sections.

Results

Vector Design and Strategy for Trans-Splicing rAAV Vectors. Based on our previous findings that the mechanisms of rAAV transduction involve circular concatamerization (7, 8, 10), we hypothesized that a dual vector approach could be used to deliver a functional genomic locus exceeding the packaging capacity of a single AAV virion. Inherent in the design of this approach is an assumption that intermolecular concatamerization will allow for

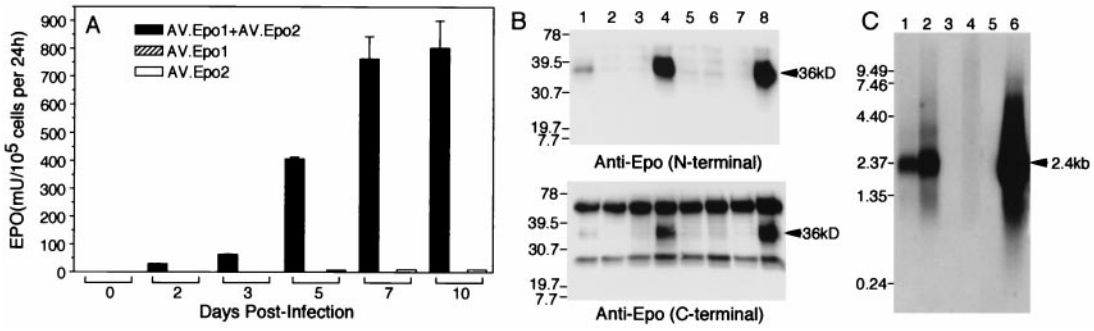

Fig. 2. Production of Epo protein after coinfection of primary fibroblasts with two independent trans-splicing vectors. Confluent primary fetal fibroblasts (8×10^5 cells) were infected with 7×10^9 particles each of AV.Epo1 and/or AV.Epo2 viral vectors. Epo expression was monitored using ELISA by harvesting culture media 24 h subsequent to media replacement. (*A*) Results comparing the indicated three vector combinations give the mean (±SEM) Epo levels from three independent experiments normalized to 1×10^5 cells. (*B*) Samples of fibroblast culture media (1 ml) at 2 days (lanes 1–3) and 10 days (lanes 4–6) postinfection with either AV.Epo1/AV.Epo2 (lanes 1 and 4), AV.Epo1 (lanes 2 and 5), or AV.Epo2 (lanes 3 and 6) were immunoprecipitated with a rabbit polyclonal anti-human Epo Ab (R&D Systems) and resolved by 12% SDS/PAGE. Western blots were then probed with either an N-terminal (*Upper*) (Santa Cruz Biotechnology) or C-terminal (*Lower*) (R&D Systems) anti-Epo Ab and detected by ECL. Lanes 7 and 8 represent mock-infected and control cells infected with a full-length cDNA Epo AAV vector, respectively. Arrows indicating the glycosylated Epo protein (36 kDa) and molecular mass markers (kDa) are to the left of each blot. (*C*) Northern blot analysis of Epo mRNA expression: lane 1, coinfected with AV.Epo1/AV.Epo2 (5 days); lane 2, coinfected with AV.Epo1/AV.Epo2 (10 days); lane 3, infected with AV.Epo1 alone (10 days); lane 4, infected with AV.Epo2 alone (10 days); lane 5, uninfected; lane 6, transfected with pEpoEGFP (as a control for the full-length Epo/EGFP bicistronic message). Molecular lengths (kb) are marked to the left of the gel. Successful transcription and splicing will yield a 2.28-kb mature mRNA + poly(A) tail (marked by arrow at 2.4 kb).

positionally correct exon/intron splicing when two independent viral genomes are juxtaposed within a circular concatamer. To test this hypothesis, we designed two independent vectors (AV.Epo1 and AV.Epo2), each encoding a portion of the Epo gene complete with intact endogenous splicing signals (Fig. 1*A*). Additionally, two different bacterial selectable markers (Kan^r and Amp^r genes) were placed in the two vectors, and a bacterial origin of replication was placed only in AV.Epo1. These bacterial elements allow for rescue and structural analysis of circular concatamers after transformation of low molecular weight Hirt DNA from infected cells into bacteria. Last, to aid in the direct visualization of correctly spliced messages, an IRES sequence was placed 3′ to Epo exon 5, followed by the EGFP gene. Using this vector design, we hypothesized that a certain percentage of circular concatamers should be in the head-to-tail orientation diagrammed in Fig. 1*B*. If indeed transcription of heterogeneous nuclear RNA through the junctional ITRs was efficient, we would expect to visualize functional transcripts expressing both Epo and EGFP protein only after correct splicing (Fig. 1*C*).

Trans-Splicing Epo Genomic Vectors Express Epo Protein *in Vitro*. We initially tested this vector system *in vitro* on confluent monolayers of fetal fibroblast cells. As with muscle, these cells have been previously shown to produce circular intermediates during latent infection with rAAV (14). Fibroblast monolayers were infected at a multiplicity of infection of 10,000 particles per cell with each of the Epo vectors alone or in combination. Expression of Epo protein was first analyzed at various times postinfection by ELISA using a C-terminal capture Ab. Additionally, Northern blots characterized the size of Epo transcripts, and Western blots with both anti-Epo N-terminal and anti-Epo C-terminal Abs characterized the Epo protein. Results from these analyses are shown in Fig. 2. Epo protein expression in fibroblasts coinfected with both AV.Epo1 and AV.Epo2 demonstrated a time-dependent increase concordant with the known time course for circular concatamerization from rAAV genomes (Fig. 2*A*) (14). Although Epo levels were much higher when both vectors were administered to cells simultaneously, a very low level of immunoreactivity was seen in cells treated with AV.Epo2 but not AV.Epo1 vector. Presumably this background signal resulted from transcription initiated within the ITR, leading to a truncated Epo protein that reacted with the C-terminal Ab used in ELISA. To confirm that Epo detected by ELISA from AV.Epo1/AVEpo2 coinfected cultures originated from full-length Epo mRNA, both Northern and Western blots were performed on infected fibroblasts. Results from these studies demonstrate that only full-length Epo protein (Fig. 2*B*) and mRNA (Fig. 2*C*) were detected in cultures coinfected with both viral vectors. Hence, the low level of Epo ELISA immunoreactive material seen in fibroblasts infected with AV.Epo2 alone was below the sensitivity for detection by both Northern and Western blots. In summary, these results support our original hypothesis that the concatamerization of rAAV genomes can be used to express genes exceeding the packaging capacity of AAV by means of trans-splicing between two independent vectors.

Functional Expression of Epo *in Vivo* by Using a Dual Vector Trans-Splicing Approach. With the knowledge that circular concatamerization is intricately linked to the rAAV latent life cycle in muscle (7, 10), we next sought to test whether this trans-splicing approach would be effective *in vivo*. Furthermore, this *in vivo* model would allow for functional confirmation of Epo expression based on physiologic changes in hematocrit. To this end, the tibialis muscles in 4- to 6-wk-old C57BL6 mice were infected with AV.Epo1 and/or AV.Epo2, and changes in hematocrit were evaluated over the course of 110 days. Experimental conditions used to evaluate trans-splicing events involved the simultaneous delivery of an equivalent amount of each vector to the same muscle. Two doses used for evaluation were 6×10^{10} or 4×10^{11} total viral particles per muscle. Control muscles were infected with either AV.Epo1 or AV.Epo2 alone. Age-matched, uninfected control mice also served to establish a baseline in these assays. As shown in Fig. 3*A*, only muscle samples coinfected with both AV.Epo1 and AV.Epo2 gave rise to a statistically significant ($P < 0.001$) time-dependent increase in the hematocrit, from a baseline of 48% in control animals to as high as 86% in the high dose animals. Similarly, serum levels of human Epo, as determined by ELISA, demonstrated immunoreactivity only in animals coinfected with both viruses in the same muscle (Fig. 3*B*). This time-dependent increase in muscle Epo expression, indicated by both hematocrit and ELISA, mirrored the time-dependent concatamerization process previously demonstrated with molecular endpoints in muscle (7, 10). According to the vector design, if the correct head-to-tail concatamer was formed in cells infected with both vectors, we would expect to also see IRES-mediated EGFP expression derived from transcription initiated from the cytomegalovirus (CMV) promoter of AV.Epo1. To

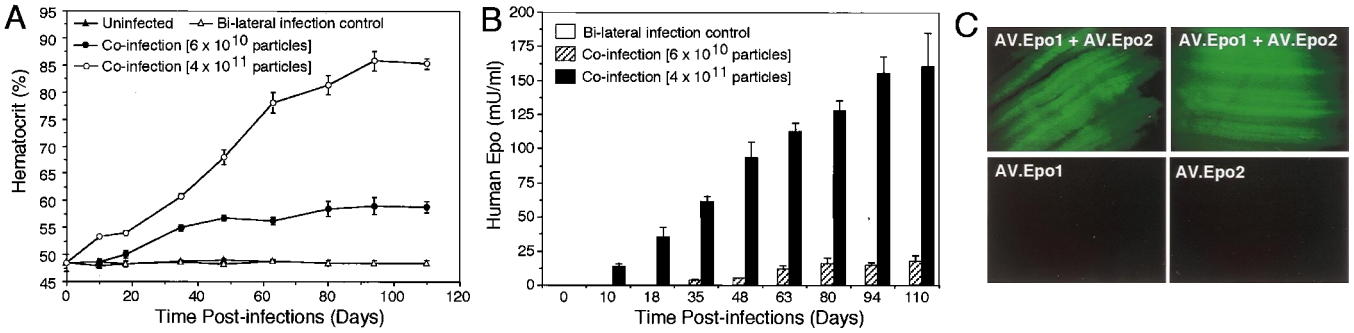

Fig. 3. *In vivo* production of Epo protein from trans-splicing rAAV vectors in muscle. The tibialis muscles of C57BL6 mice were injected with either 6×10^{10} particles or 4×10^{11} particles by direct coinfection with both AV.Epo1 and AV.Epo2 or bilateral infection of tibialis muscles with each vector individually. Uninfected age-matched controls were also evaluated at the same time. Hematocrits were analyzed by retroorbital bleeding (*A*), and serum levels of human Epo protein were evaluated by using a human-specific ELISA protocol (*B*) at various times postinfection. No changes in hematocrit or the level of human Epo protein were detected in animals infected with the individual vectors in separate tibialis muscles (only data for the high dose group are shown). Results depict the mean (±SEM) for $n = 6$ (virally coinfected low dose group), $n = 4$ (virally coinfected high dose group), and $n = 4$ (control groups) independent animals in each group. (*C*) EGFP expression in AV.Epo1- and/or AV.Epo2-infected muscles at 150 days postinfection. Images show representative fluorescent photomicrographs of whole mount fresh muscle tissues.

investigate this issue, we examined EGFP expression in whole mounts of the freshly harvested muscles at 150 days postinfection. As shown in Fig. 3*C*, EGFP expression was detected only in muscles coinfected with both AV.Epo1 and AV.Epo2.

Molecular Identification of Epo-Expressing Intermolecular Circular AAV Concatamers in Muscle. To elucidate the structural organization of the intermolecular recombinants responsible for Epo expression *in vivo*, AAV circular intermediates were rescued from Hirt DNA prepared from infected muscle samples, and Amp^r plasmids were propagated in bacteria before structural and functional analysis. Initial screens for the abundance of intermolecular concatamers involved colony hybridization of Amp^r clones against probes contained within the AV.Epo1 or AV.Epo2 vectors (Fig. 1). These data, which are summarized in Table 1, demonstrate that intermolecular concatamers accounted for 36–37% of rescued circular intermediates by 110–150 days only in muscles coinfected with AV.Epo1 and AV.Epo2. Furthermore, the percentage of intermolecular circular concatamers identified by hybridization closely mirrored the percentage of Amp^r/Kan^r co-resistant rescued plasmids at these time points (Table 1). To exclude any potential artifactual intermolecular recombination that might originate within the host bacteria, Hirt DNA samples purified from muscles at 110 days postinfection with either AV.Epo1 or AV.Epo2 were combined and cotransformed into host bacteria simultaneously. No Kan^r clones originated from these experiments, when either sequential or simultaneous Amp/Kan selective pressure was applied. Taking these results together with previous reports demonstrating the lack of bacterial-mediated circularization of linear AAV genomes (7, 8), we are confident that intermolecular concatamerization in this model is mediated by *in vivo* cellular processes.

Detailed Southern blot analyses using EGFP, 5′Epo, and 3′Epo probes were performed on 92 clones that hybridized to both vector probes in colony hybridization assays and 10 clones that hybridized only to the 5′ Epo probe. Three typical clones are shown in Fig. 4. These clones include an AV.Epo1-derived circular monomer (p21) and circular concatamers derived from both AV.Epo1 and AV.Epo2 in either head-to-tail (p16) or head-to-head orientation (p19) (Fig. 4 *A* and *B*). Diagnostic restriction fragments after *Kpn*I and *Afl*III digestion included a single 4.7-kb band for p21 that hybridized to the 5′Epo probe (consistent with circular monomer of AV.Epo1), a 2.3-kb *Kpn*I junctional fragment for p16 that hybridized to both 5′ and 3′ Epo probes (consistent with a head-to-tail dimer between AV.Epo1 and AV.Epo2), and a 3.9-kb *Kpn*I junctional fragment for p19 that hybridized to both 5′ Epo and EGFP probes (consistent with a head-to-head dimer between AV.Epo1 and AV.Epo2). Additional restriction digestions and Southern blot hybridization patterns also support the proposed circular intermediate structures presented in Fig. 4*B*.

Table 1. Circular AAV genomes rescued from rAAV-infected muscle

Vector	Viral dose*	E1-positive cfu†	E1/E2-positive cfu†	% E1-positive also E2-positive‡	% E1/E2-positive also Amp^r/Kan^r	%§ Amp^r also Kan^r	Kan^{r}Amp^r head-to-tail¶	Kan^{r}Amp^r head-to-head¶
E1/E2	6×10^{10}	8,671 ± 483	3,208 ± 148	36 ± 3.1	100	29 ± 2.8	10/36	15/36
E1	6×10^{10}	10,956 ± 401	0	0	0	0	—	—
E2	6×10^{10}	0	0	0	0	0	—	—
E1/E2	4×10^{11}	27,159 ± 6,031	11,317 ± 3,398	37 ± 4.8	100	32 ± 4.4	16/56	9/56
E1	4×10^{11}	26,800 ± 713	0	0	0	0	—	—
E2	4×10^{11}	0	0	0	0	0	—	—

*Samples were harvested at 110 days (low dose) and 150 days (high dose), and three muscle samples were analyzed for each experimental condition.

†Hirt DNA was prepared, and Amp^r colonies were rescued by transformation into bacteria. Colony hybridization was performed against DNA probes from regions of AV.Epo1 (E1) and AV.Epo1 (E2) on 100 Amp^r colonies from each experimental sample point. The total colony-forming units (cfu) from each muscle sample were then calculated from the percentage of E1 and/or E2 hybridizing colonies and the total cfu count (mean ± SEM, $n = 6$).

‡Calculated from paired values of individual data points (mean ± SEM, $n = 6$).

§Amp^r/Kan^r colonies were determined by replica plating of 100 Amp^r colonies onto kanamycin-containing media from each time point (mean ± SEM, $n = 6$).

¶Numbers of head-to-tail or head-to-head genomes were determined by Southern blot analysis of Kan^{r}Amp^r-rescued clones from Hirt DNA. Twenty-four of the 26 plasmids with evidence of head-to-tail conformation expressed both Epo and EGFP when transiently transfected into HeLa cells. None of the head-to-head genomes expressed Epo or EGFP when transfected into HeLa cells. The remaining rescued circular intermediates had either mixed (head-to-tail and head-to-head) orientations consistent with large multimer concatamers or structures not easily identifiable with the present restriction enzymes used [i.e., could contain small deletions or rearrangements as previously reported for large multimer circular concatamers (10)].

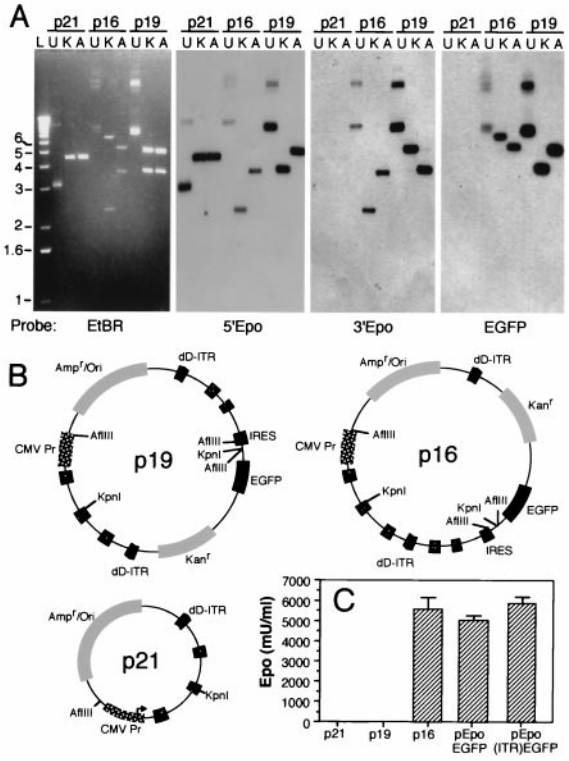

Fig. 4. Structural and functional analysis of rescued circular AAV intermediates from infected muscle. Hirt DNA was extracted from AV.Epo1- and AV.Epo2-coinfected muscles at 110 days postinfection and used to transform *E. coli*. Rescued circular intermediate clones were evaluated by restriction enzyme mapping and Southern blotting against three ^{32}P-labeled probes (*A*). Probe sequences, as diagrammed in Fig. 1, included a 5′Epo 750-bp *Kpn*I/*Bcl*I fragment (containing exon 2 and part of intron 3 encoded in the AV.Epo1 vector), a 3′Epo 1.4-kb *Bcl*I/*Kpn*I fragment (containing part of intron 3 through the IRES sequence of AV.Epo2), and an EGFP 800-bp *Sac*II fragment. The structures of three representative rescued circular intermediate plasmids (p21, p16, and p19) are evaluated in *A*, with lanes marked as U (uncut), K (*Kpn*I-digested), and A (*Afl*III-digested). Molecular length standards (L) are shown in kb to the left of the ethidium bromide gel (EtBr). Probes used for each Southern blot are labeled below each panel. p21 was an Amp^r clone with digestion patterns consistent with a circular monomer from AV.Epo1. p19, and p16 were Amp/Kan coresistant clones with digestion patterns consistent with intermolecular dimer concatamers of AV.Epo1 and Av.Epo2 with head-to-head and head-to-tail orientations, respectively. Structures of these clones are diagrammatically depicted in *B*. These representative clones were transfected into HeLa cells to evaluate Epo expression (*C*). Epo protein was detected by ELISA assay and normalized by cotransfection with a pCMVluciferase reporter as the internal standard. pEpoEGFP (with the full-length Epo gene) and pEpo-(ITR)EGFP (derived from pEpoEGFP with a double-D ITR structure inserted into intron 3 of the Epo gene) were used as comparative positive controls. Results indicate the mean (±SEM) for three independent transfections.

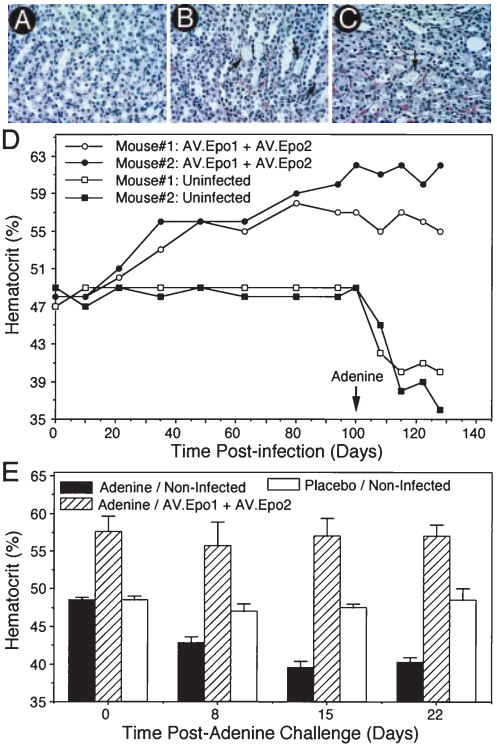

Fig. 5. Trans-splicing production of human Epo protects from adenine-induced renal failure anemia. C57BL6 mice were infected with 6×10^{10} particles of both AV.Epo1 and AV.Epo2 in the same tibialis muscle and challenged with adenine time-release capsules implanted s.c. at 35 or 100 days postinfection. Both adenine-treated/uninfected and placebo-treated/uninfected age-matched animals were also evaluated as controls. Hematoxylin/eosin sections (8 μm) of kidneys from placebo-treated/uninfected (*A*), adenine-treated/uninfected (*B*), and adenine-treated AV.Epo1/AV.Epo2 coinfected (*C*) mice are shown. Comparison of *A* with *B* and *C* demonstrates significant cast formation (arrow) in proximal tubules in both adenine-treated groups. In contrast, as shown in *D*, animals infected with both AV.Epo1 and AV.Epo2 were provided with significant protection from adenine-induced anemia initiated at 100 days postinfection (arrow). Viral infection was performed at day 0. (*E*) Mean (±SEM) hematocrit from both combined groups (n = 4 for each condition) for placebo-treated/uninfected, adenine-treated/uninfected, and adenine-treated/AV.Epo1/AV.Epo2 coinfected animals. In the adenine treatment groups of these combined data, 4 animals were challenged at both 35 (n = 2) and 100 (n = 2) days postinfection with AV.Epo1 and AV.Epo2.

To correlate functional capacity to express Epo with the determined structure of rescued circular intermediates, we performed transfection experiment in HeLa cells. Results evaluating the three rescued plasmids discussed above are shown in Fig. 4*C*. Expression of both Epo and EGFP was achieved only in cells transfected with p16, confirming that directional intermolecular concatamerization in a head-to-tail orientation is necessary for functional expression of Epo. In a larger set of plasmids with structure similar to that of p16, 24 of 26 plasmids analyzed by transfection also expressed Epo and EGFP. In contrast, of the 24 plasmids with intermolecular structure similar to that of p19, none expressed detectable levels of Epo or EGFP. As comparative positive controls, two plasmids, pEpoEGFP and pEpo(ITR)EGFP, which contained the intact Epo genomic transgene and IRES EGFP sequences used in our vector, were also evaluated for functional expression of Epo (Fig. 4*C*). These constructs differ by the insertion of a double-D ITR sequence in intron 3 of pEpo(ITR)EGFP. Interestingly, Epo expression from these control plasmids was equivalent, suggesting that the palindromic double-D ITR structures associated with junctional sequences in circular concatamers (9) do not affect transcription through the Epo gene.

Intermolecular Trans-Splicing Produces Therapeutic Levels of the Epo Protein Capable of Protecting Mice from Renal Failure-Induced Anemia. Based on the above findings, we were encouraged that trans-splicing between two independent AAV vectors could generate a full-length functional Epo gene from genomic fragments *in vivo*. However, it was critical to determine whether the levels of protein expression achieved by this approach could be therapeutically useful. For this evaluation, the experimental strategy was to determine whether the level of Epo produced by this approach was capable of protecting animals from anemia produced by adenine toxicity to the kidney (15). This model of adenine-induced chronic renal failure, which primarily affects the proximal tubules and glomeruli, has been demonstrated to substantially affect hemato-

poietic function, and to reduce both the Epo level and the hematocrit in rats (15, 16). In our experiments, animals were coinfected with a total of 6×10^{10} particles per muscle of AV.Epo1 and AV.Epo2, 35 and 100 days before adenine challenge. To produce anemia, mice received time-release tablets of adenine delivering 25 μg per gram body weight per day. Control groups consisted of age-matched animals treated with adenine or placebo tablets, but not infected with virus. As shown in Fig. 5 *B* and *C*, adenine treatment produced renal pathology, as evident by cast formation in proximal tubules, as well as obvious tubular and glomerular swelling (data not shown). This pathology was seen in both virally infected and uninfected groups treated with adenine (Fig. 5 *B* and *C*), but not in placebo-treated animals (Fig. 5*A*). However, animals preinfected with both AV.Epo1 and AV.Epo2 at 100 days before adenine challenge were significantly protected from anemia (Fig. 5*D*). In contrast, uninfected control animals demonstrated a significant decrease in hematocrit by 21 days after the initiation of the adenine challenge. Combined data from both 35-day and 100-day preinfected animals are shown in Fig. 5*E*. These results demonstrate protection from anemia only in animals infected with both vectors. Placebo-treated, noninfected animals demonstrated no significant change in hematocrit (Fig. 5*E*), or in renal toxicity as determined by histopathology (Fig. 5*A*). In conclusion, these data demonstrate that the level of Epo protein expressed from independent trans-splicing vectors jointly encoding the human Epo genomic locus is sufficient to functionally protect mice from renal failure-induced anemia.

Discussion

Although rAAV vectors have demonstrated tremendous promise for muscle-directed gene therapies, the extensive use of these vectors is strictly limited by the relatively small packaging size ($\approx$5 kb) of the viral genome. In the present study, we have exploited the molecular mechanisms of rAAV transduction that lead to intermolecular circular concatamerization to enable the delivery of a large transgene insert by coinfection with two independent trans-splicing vectors. We demonstrated that functional expression of Epo protein can be achieved after coinfection of fibroblasts and muscle with two vectors encoding separate regions of the human genomic Epo locus. The levels of Epo protein and the rise in hematocrit produced after coinfection with AV.Epo1 and AV.Epo2 in muscle demonstrated a time-dependent increase correlating with the time-dependent processes of intermolecular concatamerization of circular AAV genomes reported previously (7, 10). Furthermore, the percentage of circular intermolecular circular concatamers from AV.Epo1 and AV.Epo2 formed in muscle by 110–150 days in our studies (36–37%, Table 1) closely mirrors that recently determined by our laboratory (30% by 100 days) in experiments using two vectors encoding either EGFP or alkaline phosphatase transgenes (10). Although our data currently suggest that a large fraction of intermolecular rAAV circular concatamer genomes in muscle remains episomal, we cannot formally exclude the possibility that some observed Epo expression in muscle is due to recombination and splicing of two rAAV genomes randomly integrated in the same chromosome. However, successful retrieval of episomal head-to-tail concatamers and subsequent functional expression of Epo in HeLa cells suggest that intermolecular trans-splicing between circular viral genomes is at least partially responsible for the observed Epo production *in vivo*.

Several factors could potentially affect the efficiency of the proposed trans-splicing approach. First, one might reason that palindromic ITR sequences found at the junctions of concatamers could inhibit transcription of heterogeneous nuclear RNA. However, reconstitution studies placing a double-D ITR within intron 3 of the Epo gene expression plasmid demonstrated that an internal ITR sequence does not inhibit read-through transcription. Second, the efficiency of this trans-splicing vector approach will undoubtedly be influenced by the dose of virus used for infection. It follows that higher doses of virus should increase the probability of intermolecular concatamerization. In support of this hypothesis, animals receiving a 6-fold higher dose of both vectors exhibited substantially higher changes in hematocrit (86%) as compared with the low dose group (59%) at 110–115 days postinfection. Furthermore, Epo protein levels were 9.4-fold higher in the high dose as compared with the low dose group at 110 days postinfection. These findings suggest that incremental increases in the infectious titer have near linear effects on increasing the efficiency of intermolecular concatamerization. Thus, the efficiency of this dual vector strategy should benefit from improved techniques for generating higher titers of virus.

Last, we have demonstrated that Epo levels generated by dual vector infection and trans-splicing in muscle are functionally capable of protection from anemia induced by renal failure. Epo expression is predominantly regulated by the peritubular, capillary lining cells of the kidney (17). In kidney failure, decreased Epo expression leads to a substantial decline in hematocrit (18). Because serum levels of Epo protein are generally thought not to affect adenine-induced renal toxicity, it is not surprising that both virally infected and noninfected animals treated with adenine have similar extents of renal histopathology.

The implications of these findings for gene therapy using AAV vectors are quite significant. They suggest that, in principal, two independent vectors encoding large transgenes in two segments flanked by the proper splicing sequences can be used to deliver therapeutic proteins. One can envision that this strategy could be used to overcome several distinct disadvantages of the small packaging size of AAV. First, large cDNAs could be engineered with heterologous splice sites and delivered in two independent vectors. A second potentially useful extension of this methodology could be the incorporation of large intact genes with intronic splice site sequences and regulatory elements in a context similar to the endogenous locus. This approach could be beneficial for genes demonstrating complex regulatory or splicing patterns that are required to complement a disease state. In summary, the development of this trans-splicing approach for rAAV should significantly increase the utility of this vector for gene therapies of inherited and acquired diseases.

This work was supported by National Institutes of Health Grant RO1 HL58340 and the Gene Therapy Core Center, cofunded by the National Institutes of Health and the Cystic Fibrosis Foundation (P30 DK54759).

1. Muzyczka, N. (1992) *Curr. Top Microbiol. Immunol.* **158,** 97–129.
2. Carter, B. J. (1992) *Curr. Opin. Biotechnol.* **3,** 533–539.
3. Berns, K. I. & Giraud, C. (1996) *Adeno-Associated Virus (AAV) Vectors in Gene Therapy* (Springer, Berlin).
4. Summerford, C. & Samulski, R. J. (1998) *J. Virol.* **72,** 1438–1445.
5. Summerford, C., Bartlett, J. S. & Samulski, R. J. (1999) *Nat. Med.* **5,** 78–82.
6. Qing, K., Mah, C., Hansen, J., Zhou, S., Dwarki, V. & Srivastava, A. (1999) *Nat. Med.* **5,** 71–77.
7. Duan, D., Sharma, P., Yang, J., Yue, Y., Dudus, L., Zhang, Y., Fisher, K. J. & Engelhardt, J. F. (1998) *J. Virol.* **72,** 8568–8577.
8. Duan, D., Sharma, P., Dudus, L., Zhang, Y., Sanlioglu, S., Yan, Z., Yue, Y., Ye, Y., Lester, R., Yang, J., Fisher, K. J. & Engelhardt, J. F. (1999) *J. Virol.* **73,** 161–169.
9. Duan, D., Yan, Z., Yue, Y. & Engelhardt, J. F. (1999) *Virology* **261,** 8–14.
10. Yang, J., Zhou, W., Zhang, Y., Zidon, T., Ritchie, T. & Engelhardt, J. F. (1999) *J. Virol.* **73,** 9468–9477.
11. Samulski, R. J., Chang, L. S. & Shenk, T. (1987) *J. Virol.* **61,** 3096–3101.
12. Duan, D., Fisher, K. J., Burda, J. F. & Engelhardt, J. F. (1997) *Virus Res.* **48,** 41–56.
13. Clark, K. R., Liu, X., McGrath, J. P. & Johnson, P. R. (1999) *Hum. Gene Ther.* **10,** 1031–1039.
14. Sanlioglu, S., Duan, D. & Engelhardt, J. F. (1999) *Hum. Gene Ther.* **10,** 591–602.
15. Yokozawa, T., Zheng, P. D., Oura, H. & Koizumi, F. (1986) *Nephron* **44,** 230–234.
16. Qu, N., Wen, J. K. & Li, E. (1995) *Chung Kuo Chung Hsi I Chieh Ho Tsa Chih* **15,** 222–224.
17. Adamson, J. W. (1996) *Am. J. Med.* **101,** 4S–6S.
18. Zhang, F., Laneuville, P., Gagnon, R. F., Morin, B. & Brox, A. G. (1996) *Exp. Hematol.* **24,** 1469–1474.